Supplementary Material for

"Somatostatin, neuronal vulnerability and behavioral emotionality"

Li-Chun Lin, PhD[1] and Etienne Sibille, PhD[1-2]

[1]Department of Psychiatry, Translational Neuroscience Program, Center for Neuroscience, University of Pittsburgh, Pittsburgh, PA 15219

[2]Campbell Family Mental Health Research Institute, Centre for Addiction and Mental Health, Departments of Psychiatry, Pharmacology and Toxicology, University of Toronto, Toronto, ON, Canada

Correspondence: Dr. E Sibille, Center for Addiction and Mental Health (CAMH), 250 College street, Room 134, Toronto, ON M5T 1R8, Canada. E-mail address: Etienne.sibille@camh.ca; Phone: 416-535-8501 xt36751

Experimental Procedures

Animals. The use of animals, including all treatments, was conducted in compliance with the NIH laboratory animal care guidelines and with protocols approved by the Institutional Animal Care and Use Committee of the University of Pittsburgh. All mice were on the C57BL/6J background. All experiments were performed with 3- to 5 month-old male and female mice littermates, between 9 am and 3 pm. All non-stressed control mice were group housed and maintained under standard conditions (12/12-hour light/dark cycle, lights on at 07:00 h, 22±1°C, with food and water *ad libitum*). The Sst^{KO} mouse line was obtained from the Jackson Laboratory (stock no. 008117).[1] Sst^{KO}, Sst^{HZ}, Sst^{WT} littermates were generated by crossing Sst^{HZ} mice. Genotyping was done by Polymerase Chain Reaction (PCR) analysis of DNA isolated from tail cuts. For SST-GFP mice, the mouse line carrying a somatostatin promoter-driven Cre recombinase expression (SST-ires-cre knock-in homozygous mice; Jackson Laboratory; stock no.013044) was crossed with a Rosa^{GFP-}

floxed reporter mouse line carrying a loxP-flanked STOP cassette (Ai6 Rosa26-loxP-STOP-loxP-ZsGreen; Jackson Laboratory; stock no. 008242), as described previously [2].

Unpredictable chronic mild stress (UCMS). Mice were subjected to six weeks of a random schedule consisting of 1-3 environmental stressors per day, seven days per week.[3] Stressors included repeated bedding change, no bedding, reduced housing space, forced bath (~2 cm of water in cage), wet bedding, aversive smell (exposure to fox or bobcat urine), social stress (rotate mice into previously occupied cages or single-housing), 45° tilted cage, and mild restraint (50-ml falcon tube with air hole). Weekly assessment of weight and fur was performed to monitor physiological progression of the UCMS syndrome. The social isolation treatment began from the fifth week of UCMS until the day of euthanasia.

Behavior. Anxiety/depressive-like behaviors were tested in the elevated plus maze (EPM), open field (OF), novelty suppressed feeding (NSF), and sucrose preference test (SP) in the following order for each mouse: EPM, OF, NSF, SP, separated by a minimum of 1 day. All tests were performed during the light phase of the circadian cycle, between 9 am and 3 pm.

EPM. Anxiety-like behaviors and locomotion were measured in a cross maze with two open and two closed arms (30 cm x 5 cm) as previously described [4]. Entries and time spent in the open arms were recorded for 10 min to assess anxiety-like behaviors. Total number of entries in all arms was assessed as an index of locomotion.

OF. Anxiety-like behaviors and locomotion were measured in a 76 x 76 cm chamber divided in 16 even-size squares and monitored for 10 min using the Any-maze video-tracking software (Stoelting, Wood Dale, IL). Percentage of walking distance and time spent in the four center squares were assessed to evaluate anxiety-like behaviors. Total walking distance in the chamber was used as an index of locomotion.

NSF. Anxiety/depressive-like behaviors were measured for 11 min in a 76 x 76 cm chamber, with a food pellet in the bright-lit center. The drive to overcome the aversive center was increased by 16 hours of food deprivation before testing. The latency to start eating the food pellet was measured

as an index of anxiety/depressive-like behaviors. Food consumption in the home cage for six minutes after the test was used as a measure for appetite after NSF testing and food deprivation.

SP. The sucrose test was performed using a two-bottle choice test between a 2% sucrose solution and water. Mice had free access to both water and a 2% sucrose solution 48 hours before the test in their home cage to reduce neophobia. Following training, for 16 h from 18:00 pm-10:00 am (active phase) and given free access to both water and the 2% sucrose solution. Position of bottles was counterbalanced across the left and the right sides from test to test. Sucrose and water consumption were measured. Sucrose preference (percent) was calculated as follows: preference = [sucrose solution intake (ml)/total fluid intake (ml)] × 100. Sucrose consumption was calculated as: consumption = [sucrose solution intake (ml)/ body weight (g)].

Z-scoring. To assess the consistency of behavioral performance across related tests, emotionality- or locomotion- related data were normalized using a Z-score methodology [5]. Z-scores calculate the number of standard deviations (σ) a given sample (X) is above or below the mean of the control group (μ). Raw measures for EPM (time in open arm; % crosses into open arm), OF (time in center; % distance in the center), NSF (latency to feed), and SP (sucrose consumption and sucrose preference) were converted to standard deviations relative to respective means of the control group (Sst^{WT} mice). The directionality of scores was adjusted so that lower score values indicate reduced anxiety/depressive-like behaviors, and higher scores indicate heightened anxiety/depressive-like behaviors (termed emotionality). Finally, values across tests were averaged for each mouse to produce individual emotionality Z-scores. Locomotion Z-scores were similarly applied and obtained from EPM (total crosses) and OF (Total distance traveled) data.

Physiological Evaluation. The body weight and coat state of all the animals were assessed and scored (0-2 points) weekly by a double-blinded experimenter until the end of the UCMS treatment. The total score of the coat state resulted from the sum of the score of five different body parts: head, neck, dorsal and ventral fur, tails and paws. A score of 0 was given for a well-groomed fur and increased to 2 for an unkempt fur.

Corticosterone Measurements. The stress reactivity test consisted of a 30-min restraint period, corresponding to an acute, moderate stressor. The blood samplings were drawn at three time points: immediately before, during a 30-min exposure to restraint stress, as well as 60 min after ending the stress session (recovery period). The animals were restrained in a 50-ml Falcon tube with a ventilation hole and a hole in the lid for the tail. Tail blood (30 µl) was collected into a *Microtainer*® tube with Lithium Heparin (BD Vacutainer Systems, Franklin Lakes, NJ) at 10:00-14:00. Bleeding was induced by cutting the tip of the tail, and plasma was separated by centrifugation at 1200 g, 4°C for 10 min, and then stored at -80°C until use. All samples were ran in duplicate and measured by Corticosterone *ELISA* Kit (EnzoLife Sciences, Farmingdale, NY) according to the instructions of the manufacturer.

Chronic corticosterone treatment. As described previously,[6] mice were given corticosterone (35 mg/ml; Sigma-C2505, St Louis, MO, USA) dissolved in 20% cyclodextrin (Sigma H107) as their only water supply for 6 weeks. Mice show no aversion to drinking water with corticosterone.

Visualization of individual neurons in mice. For signle-cell analyses, mice were rapidly transcardially perfused with 1 ml of 1X Tris-buffered saline and 1 ml of 4% paraformaldehyde in phosphate buffer (pH 7.4) to lightly fix tissue while preserving GFP signal and RNA integrity. Cryostat sections (20 µm) were cut from coronal blocking containing cingulate cortex (between bregma +1.42 to -0.5 mm), thaw-mounted onto on polyethylene napthalate membrane coated slides (Leica Microsystems; #11505158; Bannockburn, IL, USA) that had been treated with UV at 254 nm for 30 min. Before microdissection, slides for SST neurons were dehydrated through 100% ethanol for 10 seconds. For pyramidal neurons, cryostat sections from mice with GFP-tagged SST neurons were dried briefly and stored at -80˚C. Immediately before microdissection, slides were immersed in an ethanol-acetic fixation solution, stained with thionin, dehydrated with 100% ethanol, as described previously.[7] Pyramidal neurons were visually identified based on their location and characteristic somal morphology including pyramidal shape, large size, and thick apical dendrite.

Laser microdissection and gene expression profiling. Laser microdissection was performed

using a Leica LMD6500 system (40X objective in the fluorescence mode for SST neurons or bright-field mode for pyramidal neurons). Cutting and collection steps were subsequently examined in fluorescent or bright-field mode. 100 cells collected from the mouse cingulate cortex per animal were collected in 0.5 ml microtube caps (Ambion, Foster City, CA, USA) and lysed by vortexing for 30 sec in 150 μl of RLT Buffer Plus (Qiagen, Valencia, CA, USA) within a 3-hour time span, and stored at −80 °C until further processing. Total RNA was then extracted using the RNeasy Plus Micro Kit (Qiagen) according to the manufacturer's instructions. RNA samples were amplified with NuGEN® Ovation Pico WTA System V2 (NuGen, San Carlos, CA). The fragmented labeled cDNA samples were processed and hybridized to Affymetrix® Mouse Gene 1.1 ST Array Plates (Affymetrix).

Data mining and visualization. Gene expression information was obtained with the Affymetrix console software. Genes (dataset targets) showing significant differences (Student t-test p <0.005; >1.2 fold cutoff) in expression between stressed and unstressed SST neurons were analyzed using the IPA software (Ingenuity Systems, Redwood, CA).

Canonical pathway analysis. The Ingenuity Knowledge Base has included 642 well-characterized, canonical pathways that were derived from journal articles, textbooks, and the KEGG database, all manually curated by PhD-level scientists. Canonical pathways that differed most significantly were determined by Fisher's exact test. As a result, a *p*-value was obtained for determining the probability that the association between our dataset targets and the canonical pathway can be explained by chance. In addition, a ratio was determined by the number of dataset targets that map to the pathway divided by the total number of molecules that exist in the canonical pathway.

Upstream regulator analysis. Based on previous knowledge of expected causal effects between upstream regulators/drugs and their target genes stored in the Ingenuity® Knowledge Base, this analysis predicted which upstream regulators can explain the observed alterations of our dataset targets by Fisher's exact test. As a result, a *p*-value was obtained for determining the significance of enrichment of network-regulated genes (the dataset targets downstream of an upstream

regulator).

Real-time quantitative polymerase chain reaction (qPCR). For molecular phenotypes in mice with low SST, brains were flash frozen on dry ice after sacrifice. Bilateral cingulate cortex was obtained using a cryostat and a 1-mm-bore tissue punch. Total RNA was extracted using the RNeasy Micro Kit (Qiagen) according to the manufacturer's instructions. Reverse transcription reaction was performed using the qScript cDNA Supermix (Quanta Biosciences, Gaithersburg, MD). The comparative threshold cycle (Ct) measurement was performed for quantification with SYBR green fluorescence signal (Invitrogen, Carlsbad, CA) using a Mastercycler® ep Realplex2 real-time PCR machine (Eppendorf, Westbury, NY). PCR thermal cycling was 65°C to 59°C touch-down followed by 40 cycles (95 °C for 10 sec, at 59 °C for 10 sec, and 72 °C for 10 sec). Samples were run in triplicate and the difference in cycle threshold (ΔCt) values for each GABA/BDNF-related transcript were determined by comparison to the geometric mean of three control genes (actin, GAPDH, cyclophilin). The relative expression level of each targeted transcript was determined as 2^{-dCt}.

For single-cell analyses, total RNA from mouse cells were amplified with NuGEN® Ovation Pico WTA System V2 (NuGen, San Carlos, CA). Samples were run in triplicates and the difference in ΔCt values for each transcript was determined by comparison to a non-biased control gene, neurofilament (NEFM).

RNAscope Assay for *in situ* RNA Detection

Probe sequences of mouse somatostatin conjugated to Alexa Fluor 488, and eIF2A conjugated to 546 were custom-made (Advanced Cell Diagnostics, Hayward, CA). Fresh-frozen cryostat sections (10 μm) were placed on slides and fixed in cold 4% paraformaldehyde for 1 hour, followed by dehydration in an ethanol series. Tissue sections were then dried at room temperature for 30 min, followed by protease digestion at room temperature for 10 min. Using RNAscope Fluorescent Multiplex Reagent Kit (Advanced Cell Diagnostics; # 32085), tissue sections were then rinsed in deionized water, and immediately treated with target probes, preamplifier, amplifier, and label

probe in a HybEZ hybridization oven (Advanced Cell Diagnostics, Hayward, CA) according to the instructions of the manufacturer. Images were acquired using an Olympus IX71 fluorescent microscope (Olympus, Tokyo, Japan) and a *Fast 1394* CCD *Camera* (QImaging, BC, *Canada*). Overlapping signals from different fluorophores were separated and visualized under a 20x objective lens with MetaMorph Advanced software *(Molecular Devices*, CA, USA). The ratio of overlapping fluorescent signal areas from EIF2A and SST mRNA transcripts was determined in the cingulate cortex, based on 5 microscopic images from 3 tissue sections of each animal.

Drug Administration. The selective EIF2A phosphatase inhibitor complexes, Salubrinal (Millipore, Billerica, MA, USA) and the EIF2AK3/PERK inhibitor, GSK2606414 (Millipore, Billerica, MA, USA) were dissolved in 100% dimethyl sulfoxide (DMSO) and later diluted in saline (0.9% NaCl). Based on previous studies,[8-11] vehicle (10% DMSO/saline), Salubrinal (1.5 mg/kg), and GSK2606414 (30 mg/kg) were administered by oral gavage once daily for 7 days to mice (0.1 ml/10 mg) treated with 3 weeks of UCMS before behavioral testing. Three days of booster administrations were given on the second day after each test. Concentrations were adjusted to administer 10 ml/kg. After 7 days of drug treatments, anxiety/depressive-like behaviors and locomotion were tested in the following order: EPM, NSF, OF, separated by one day of booster administration. All tests were performed during the light phase of the circadian cycle, between 9 am and 3 pm.

Statistical Analysis. Statistical analyses were carried out using GraphPrism Version 6.0 (Graph Pad. Software Inc., San Diego, CA, USA). Student's *t* test was used to compare means between two groups, and one-way or two-way analysis of variance followed by Tukey's post hoc among means were used to determine significant differences among multiple groups. All data are expressed as means ± standard error of the mean.
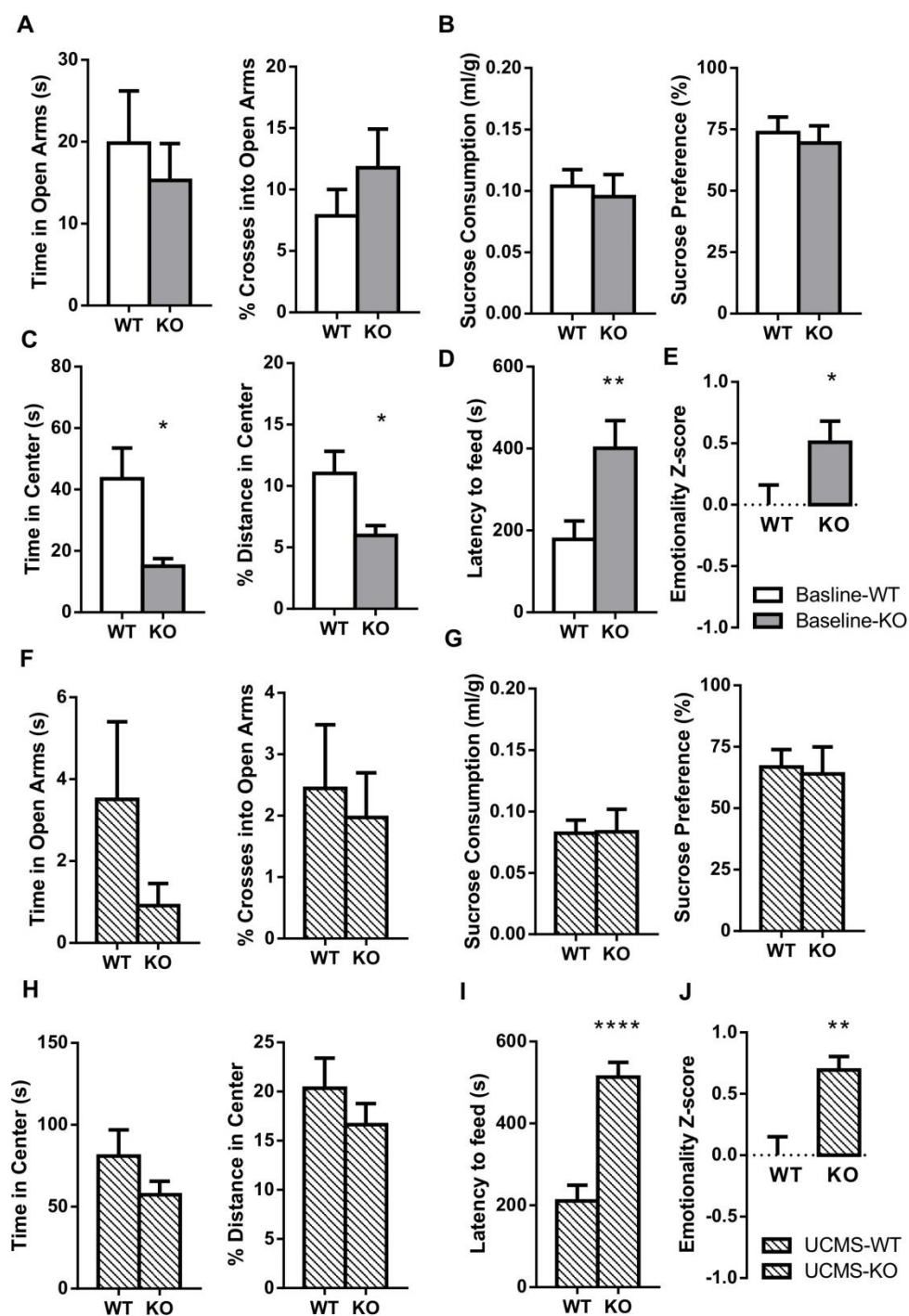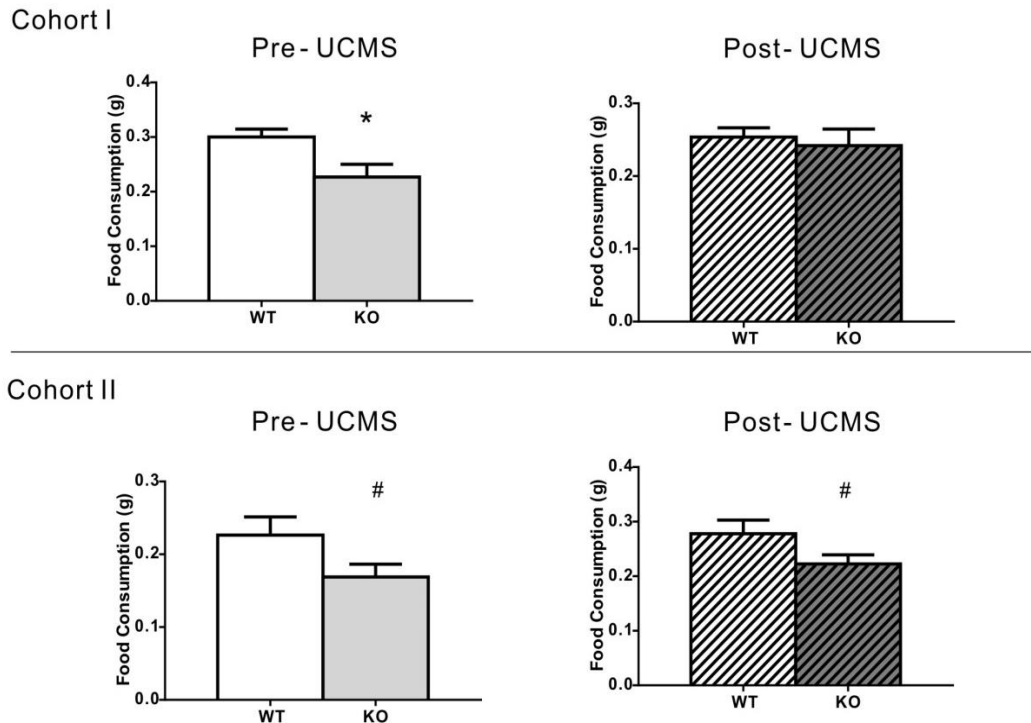
Supplemental Figure 1: Assessment of anxiety/depressive-like behaviors in *Sst^KO* mice at baseline and after UCMS. Behavioral phenotypes, including anxiety/depressive-like behaviors and overall emotionality scores in the elevated plus maze (EPM; A, F), sucrose preference test

(SP; B, G), open field (OF; C, H), and novelty suppressed feeding test (NSF; D, I) were examined in Sst^{KO} and Sst^{WT} mice at baseline and after UCMS. Overall emotionality Z scores were summarized (E, J). $*p<0.05$, $**p<0.01$, $****p<0.001$. Error bars represent the standard error of the mean. (n=12-15/group, 6-9 mice/sex).
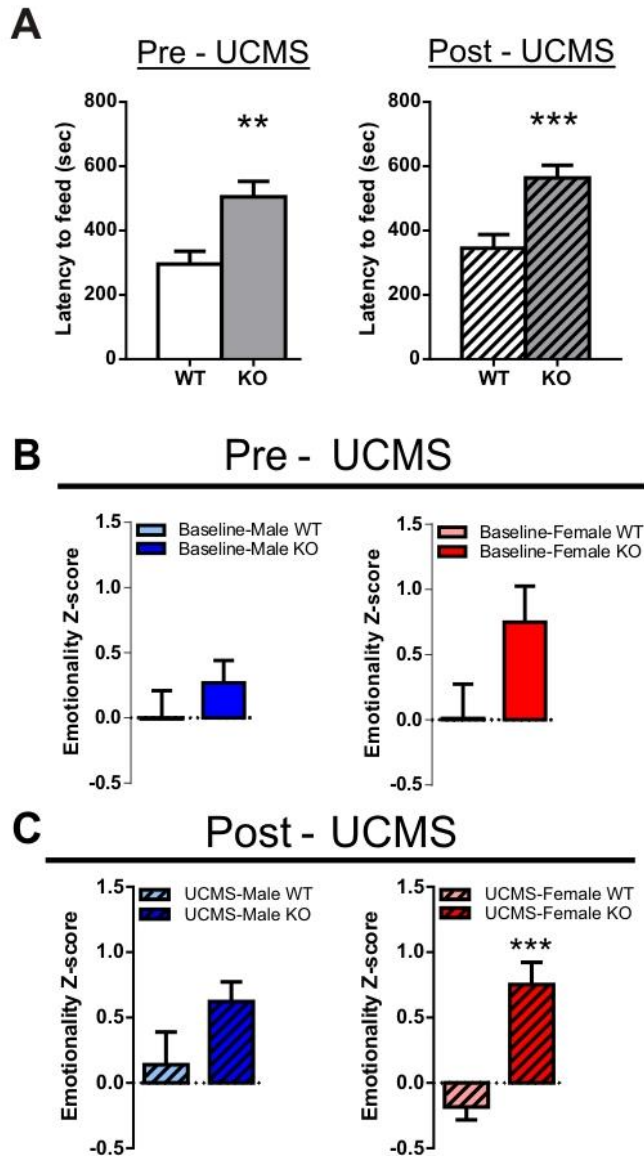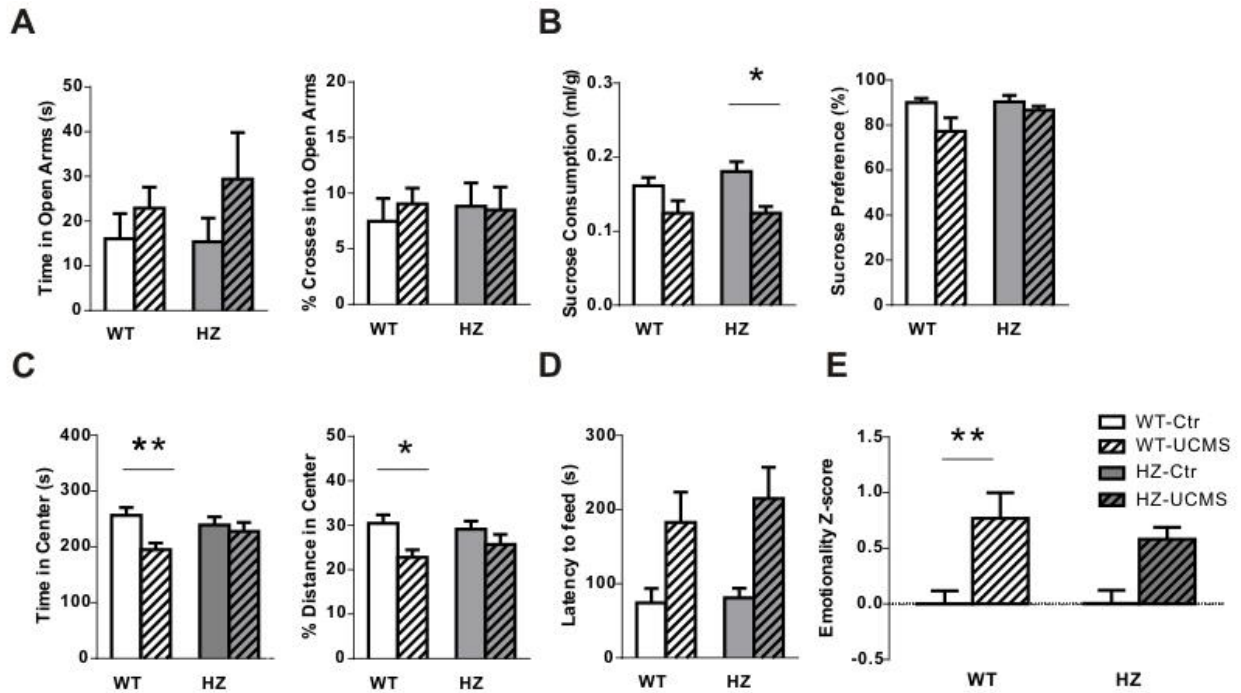
Supplemental Figure 2: Assessment of anxiety/depressive-like behaviors and potential sex differences in *Sst^KO* mice before and after exposure to chronic stress. (A) *Sst^KO* mice in a second cohort showed high anxiety/depressive-like behaviors in the novelty suppressed feeding testing at baseline (left) and after exposure to unpredictable chronic mild stress (UCMS) (right) compared to *Sst^WT* mice. (B-C) Female *Sst^KO* mice showed more robust phenotypes after chronic stress. **$p<0.01$, ***$p<0.005$. Error bars represent the standard error of the mean. (*n*=12-19/group, 6-11 mice/sex).

Supplemental Figure 3: Assessment of food consumption after 16 hours of food deprivation and NSF test in Sst^{KO} mice under non-stressed and stressed conditions. In the first cohort, non-stressed Sst^{KO} mice ate less food when they returned to their home cage after NSF testing. Stressed Sst^{KO} mice had normal food consumption when they returned to their home cage. In the first cohort, Sst^{KO} show a trend of reduced food consumption under non-stressed and stressed conditions. *$p<0.05$, #$p<0.1$. Error bars represent the standard error of the mean (n=12-19/group, 6-11 mice/sex).

A
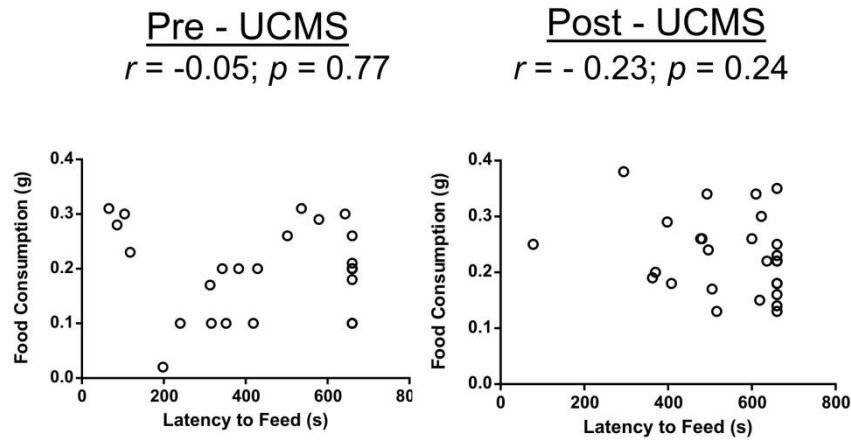
B
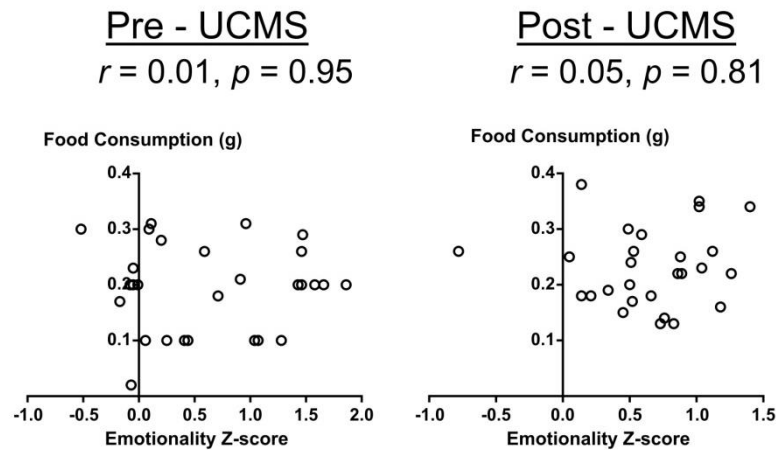
Supplemental Figure 4: No correlation between food consumption and latency in the NSF (**A**) or behavioral emotionality (**B**) in Sst^{KO} mice under non-stressed and stressed conditions. (n=12-19/group, 6-11 mice/sex).

Supplemental Figure 5: Assessment of anxiety/depressive-like behaviors in *Sst^HZ* mice under control and stressed conditions. Behavioral phenotypes, including anxiety/depressive-like behaviors and overall emotionality scores in the elevated plus maze (**A**), sucrose preference test (**B**), open field(**C**), and novelty suppressed feeding test (NSF; **D**) were examined in *Sst^HZ* and *Sst^WT* mice under control and stressed conditions. Overall emotionality Z scores (**E**) were summarized at the bottom. *$p<0.05$, **$p<0.01$, ****$p<0.001$. Error bars represent the standard error of the mean. (*n*=14 -21/genotype/treatment).
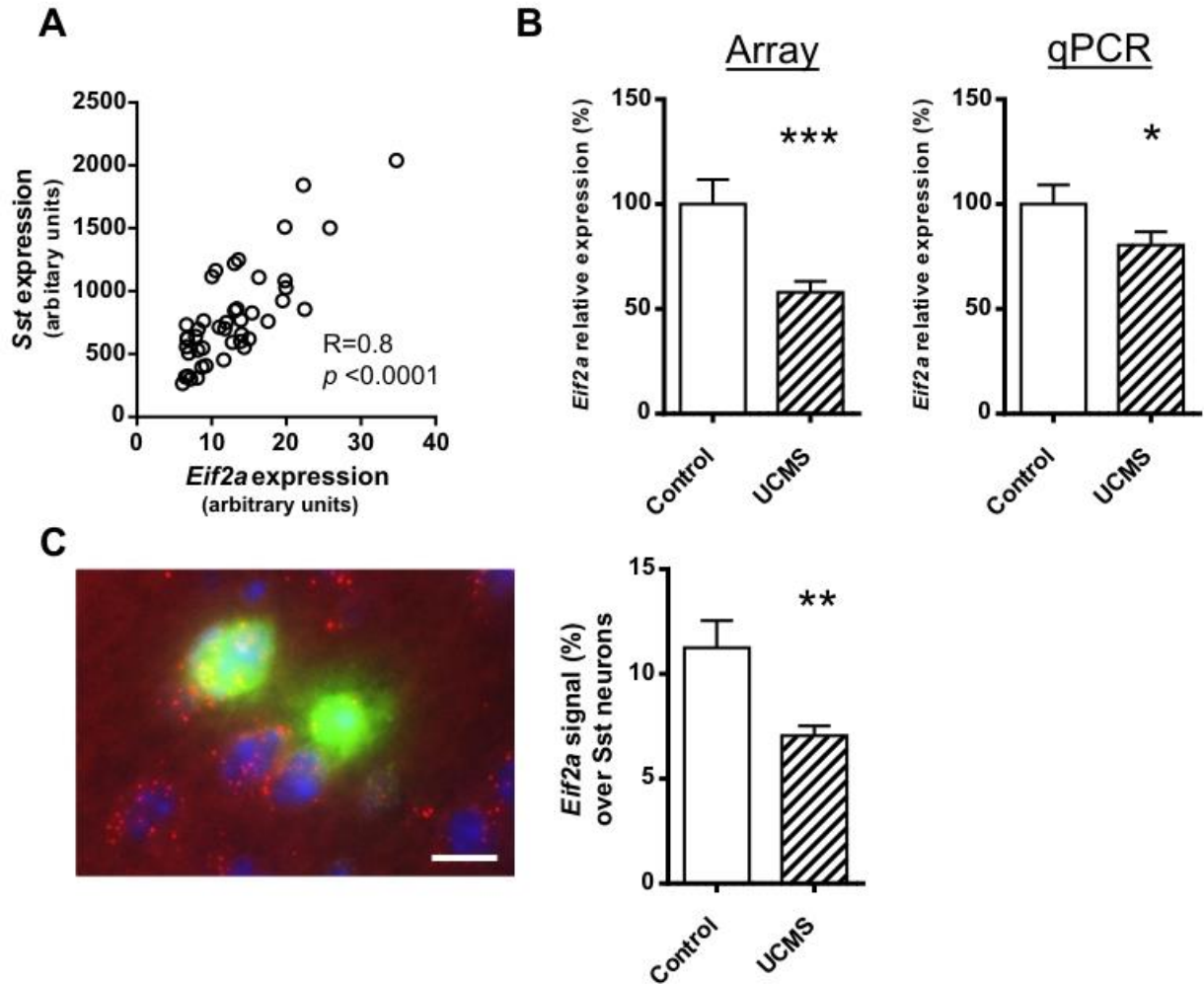
Figure S6. Validation of microarray data of *Eif2a*.

(**A**) Expression of *Eif2a* was highly correlated with SST expression in mouse SST neurons. (**B**) qPCR confirms significant down-regulation of *Eif2a* transcripts in UCMS-exposed mouse SST neurons. (**C**) Representative merged image of triple-labeling [Sst (green)/Eif2a (red)/DAPI (blue)], high-resolution RNAscope *in situ* hybridization (left). Bar represent 20 μm. Validation of the downregulation of *Eif2a* in the cortical SST cells (right). * $p<0.05$, ** $p<0.01$. Error bars represent the standard error of the mean (*n*=12-15/group).

A

Fold change
(Log$_2$ Corticosterone/Control)

R_{SST}=0.82; Slope $_{SST}$ =0.48
R_{PYR} =0.18; Slope $_{PYR}$ =0.18
K-S test p-value<2.2e-16

(Log$_2$ UCMS/Control)

● mouse SST cells
▲ mouse PYR cells

B

K-S test p-value<2.2e-16

— SST
— PYR

Frequency

Alr

C

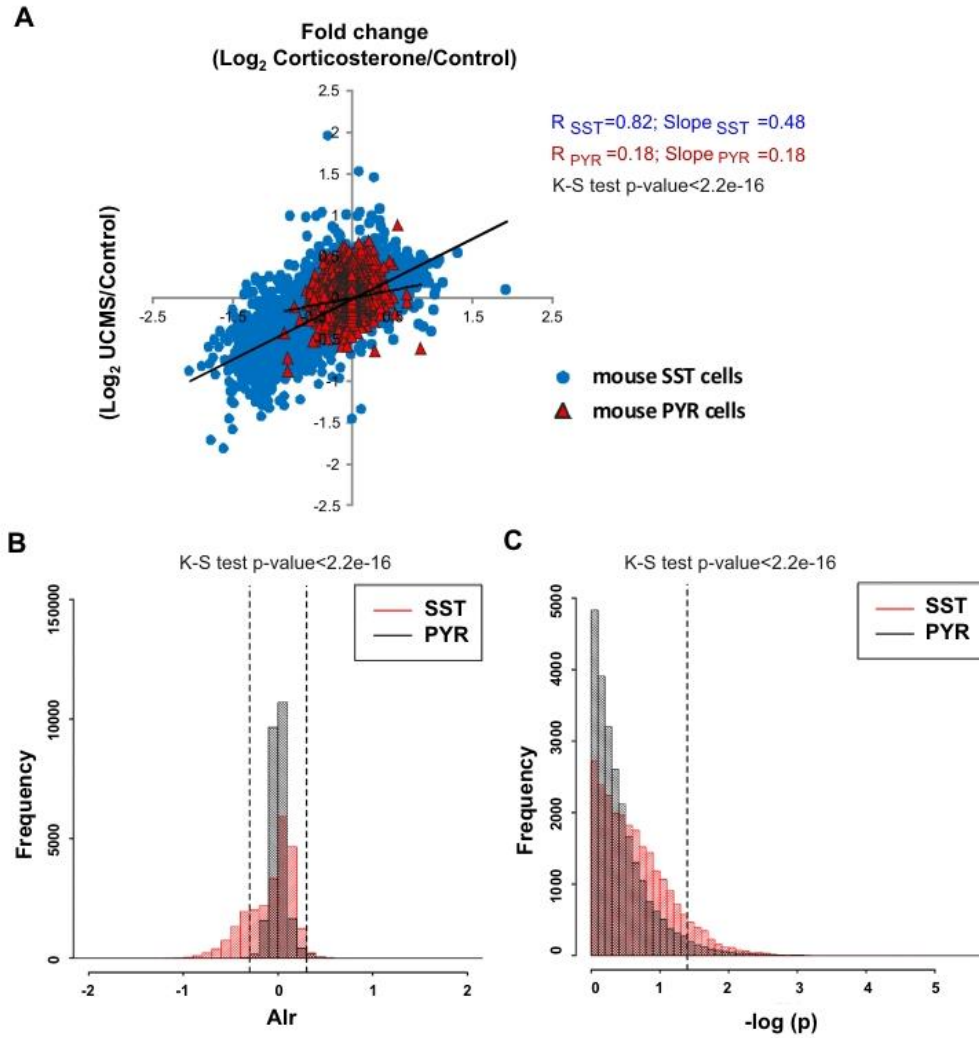K-S test p-value<2.2e-16

— SST
— PYR

Frequency

-log (p)

Figure S7: The transcriptome changes induced by chronic social/environmental or neuroendocrine stressors reflect a selective cellular vulnerability of Sst-expressing neurons. **(A)** The expression fold change of the whole transcriptome profiles in Sst-expressing neurons and pyramidal neurons (PYR) after exposure to UCMS or chronic corticosterone treatment. (**B-C**) Distributions of corticosterone effects for (**B**) effect size (<u>A</u>verage <u>l</u>og$_2$ <u>r</u>atio; Alr; changes > 20%; horizontal *dashed* lines) and (**C**) significance (*p*-value; *p* < 0.05; horizontal dashed lines) of all expressed probesets in SST neurons (red lines) and pyramidal neurons (PYR; black lines) were presented as density plots. These probability distributions between SST neurons and pyramidal neurons were significantly different. *p*-value was calculated by Kolmogorov-Smirnov (KS) test.
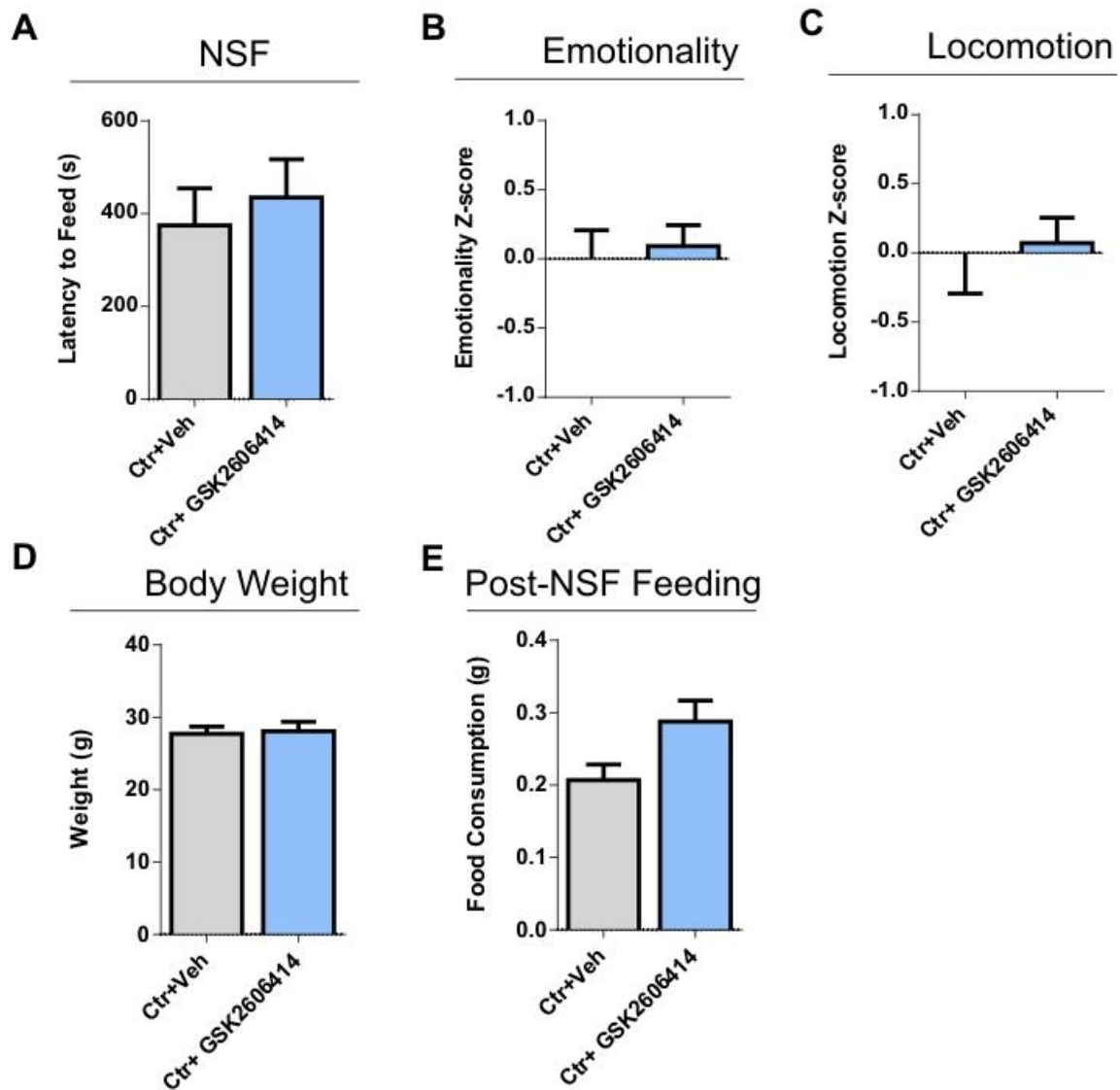
Figure S8. No phenotypes in control mice after treatment with GSK2606414, an EIF2A-mediated inhibitor of cellular stress response .

 (**A-E**) No treatments affected NSF, overall behavioral emotionality, overall locomotion, body weight, or post-NSF feeding at home cage. Error bars represent the standard error of the mean (*n*=9/group).

Supplementary Table 1. Top canonical pathways (IPA) coordinately deregulated in mouse *Sst*-expressing neurons treated with UCMS relative to non-stressed neurons.

Ingenuity Canonical Pathways	P-Value	Ratio	De-regulated Molecules [a]	
			Up	Down
Eukaryotic translation initiation factor 2	7.38E-21	40.3%	PIK3CG, INS	RPL11,RPL22,MAPK1,PIK3R1,PDPK1,KRAS,EIF3C/EIF3CL,RPS23,EIF2A,RPS7,RPS3A,EIF4G2,RPL7A,EIF3D,MAPK3,RPL19,RPL8,GSK3B,PPP1CA,RPL36A/RPL36AHNRNPH2,RPL3,RPL27,RPL37,RPL23A,EIF3E,RPLP0,RPL10A,RPL15,FAU,RPS4X,RPL39,RPS15,RPS25,RPSA,EIF3K,RPL24,PPP1CC,RPS18,RPL22L1,PPP1CB,RPS8,RPS13,RPS21,RPL35A,EIF4E,RPL7,RPL6,RPL35,RPL18A,PIK3C3,RPS9,EIF3A,AKT3,RPS5,RPL31,RPL18,MAP2K1,RPL29,RPL13,RPS24,RPL4,EIF3H,RPS2,RPL17,AGO2,RPL21,RPL23,RPL9,RPS12,EIF2S2,RPS16,RPS26,RPL28,UBA52,AGO3,EIF4A1,EIF3I,RPL38,RPS14
Oxidative Phosphorylation	8.57E-14	40.8%	COX6B2	NDUFA9,ATP5D,UQCR11,COX8A,NDUFB5,ATP5L,MTCO2,NDUFB10,NDUFA5,ATP5G1,NDUFS6,NDUFA10,ATP5F1,ATP5G3,NDUFB3,Cycs,ATP5A1,SDHC,NDUFS5,ATP5B,NDUFA6,NDUFB7,UQCRC2,COX5B,NDUFA4,COX7B,SDHB,UQCRH,COX6A1,NDUFA2,Atp5e,NDUFAB1,ATP5J2,NDUFS2,COX4I1,SDHA,NDUFV1,COX7A2,COX6B1,NDUFB4,ATP5O,NDUFV3,NDUFS3,NDUFA11,CYC1,COX5A,NDUFA3,UQCRQ
Mitochondrial Dysfunction	2.24E-12	28.8%	COX6B2, LRRK2, CPT1B	MAP2K4,NDUFA9,ATP5D,UQCR11,COX8A,NDUFB5,ATP5L,MTCO2,NDUFB10,PDHA1,NDUFA5,GPD2,ATP5G1,NDUFS6,NDUFA10,GPX4,ATP5F1,ATP5G3,NDUFB3,ATP5A1,SDHC,GSR,PRDX3,NDUFS5,ATP5B,NDUFA6,UQCRC2,NDUFB7,MAPK10,VDAC1,SNCA,COX5B,NDUFA4,COX7B,SDHB,UQCRH,COX6A1,NDUFA2,Atp5e,NDUFAB1,ATP5J2,NDUFS2,OGDH,COX4I1,SDHA,NDUFV1,NDUFB4,COX6B1,COX7A2,ATP5O,NDUFV3,MAPK8,NDUFS3,APP,NDUFA11,CYC1,COX5A,NDUFA3,UQCRQ
Remodeling of Epithelial Adherens Junctions	2.62E-09	44.3%	CDH1	NME1,RALA,RAB5B,TUBB,CLIP1,ARF6,CTNNA2,EXOC2,ARPC3,TUBA1C,CTNNB1,ACTN1,TUBB3,TUBB4B,ACTB,TUBB2A,TUBA4A,RAB7A,DNM3,ACTG1,TUBA1B,DNM1,TUBA1A,ARPC1A,ARPC2,MAPRE2,ACTN4,DNM1L,ARPC4,MAPRE3
GABA Receptor Signaling	1.00E-08	42.9%		AP2B1,AP2A1,AP2M1,ABAT,GABRA4,UBQLN1,GABBR1,Ubb,AP1B1,GABRB2,DNM1,GABBR2,NSF,SLC6A11,GAD2,GABRB3,GAD1,GABRB1,SLC6A1,GABARAP,UBC,GABRA1,GABRA2,GABRA3
Huntington's Disease Signaling	3.43E-08	26.2%	PIK3CG, GNG12	MAP2K4,MAPK1,PIK3R1,NAPG,PDPK1,Ubb,CDK5R1,GNB1,NSF,CTSD,MAPK3,DLG4,PLCB1,RASA1,GRM1,IFT57,HSPA9,CLTC,CREBBP,DNM3,GNG3,STX1A,RPH3A,ATF2,TAF9B,HDAC5,HSPA8,DYNC1I2,DNAJC5,ATP5B,HTT,POLR2I,SNCA,SDHB,PACSIN1,POLR2B,VTI1B,GNG7,EP300,POLR2A,PIK3C3,IGF1R,AKT3,PRKCE,NCOR1,NAPB,SDHA,GRIN2B,GLS,MAPK8,GNAQ,Hdac9,SNAP25,ZDHHC17,GRM5,POLR2L,DNM1,PRKCI,DCTN1,STX16,GNG5,UBC,DNM1L,PRKCB
Protein Kinase A Signaling	6.84E-08	24.0%	PTPN4, GYS2, PDE6B, TNNI2,PDE12,TCF7L1, TGFB2, PDE6G, TNNI3, TCF3, MYL10, LEF1, H2BFM, NTN1, PPP1R3D, GNG12	MYH10,MYL6,PTPN5,GNB1,CAMK2A,PLCB1,DUSP7,NFKBIB ,KDELR1,PDE2A,YWHAG,PTCH1,CREBBP,YWHAZ,PLCL2,PTP4A1,ATF2,ACP1,ANAPC5,PTPRA,CAMK2G,RAP1B,TCF4,Calm1,PTK2B,AKAP7,GNG7,EP300,AKAP11 ,PTPRJ,PRKCE,CTNNB1,PTPRT,PPP3CA,PTPN7,PTPRK,GNAQ,ADD3,ADD1,GNG5,PRKCB,PRKACB,MAPK1,YWHAH,PTEN,ROCK2,Camk2b,PPP1R7,MAPK3,PPP3R1,GSK3B,PPP1CA,YWHAE,PDE10A,YWHAB,GNG3,PTPRM,ANAPC4,H3F3A/H3F3B,MYL12B,RHOA,PTPRS,PPP1R12A,SIRPA,PPP1CC ,MYL6B,PPP1CB,PDE1A,BRAF,PPP1R10,PTPRN,MAP2K1,ADCY2,RYR2,CHP1,GNAI1 ,PDE4D,GNAI2,Ptprd,PRKCI,AKAP9,PRKAR1A
Regulation of eIF4 and p70S6K Signaling	1.21E-07	27.2%	PIK3CG	MAPK1,PIK3R1,RPS18,RPS13,RPS8,PDPK1,KRAS,RPS21,PAIP2,RPS23,EIF3C/EIF3CL,EIF4E,EIF2A,RPS7,RPS3A,EIF4G2,EIF3D,MAPK3,PIK3C3,RPS9,EIF3A,AKT3,RPS5,MAP2K1,RPS24,EIF3H,RPS2,AGO2,EIF3E,RPS12,EIF2S2,PPP2CB,FAU,RPS4X,PPP2R1A,MAPK14,RPS16,RPS26,AGO3,EIF4A1,EIF3I,RPS15,RPS25,PPP2R5E,RPS14,RPSA,EIF3K

Genes were tested for differential expression between UCMS and control groups. Statistical significance for differential expression was reached at fold-change > 20% and $p<0.005$. The resulting signature was submitted to IPA to test for over-representation of canonical pathways. The p-value was calculated by right-tailed *Fisher's exact tests* (Fisher 1922). The ratio was calculated by the number of differentially expressed genes, divided by total number of genes that make up in a given pathway.

Supplementary Table 2. Predicted Top 10 upstream regulators of transcripts affected in stressed SST neurons

Upstream regulator	*p*-value
Microtubule-associated protein tau (MAPT)	1.13E-41
Amyloid beta (A4) precursor protein(APP)	2.49E-37
Presenilin 1(PSEN1)	1.56E-30
Huntingtin (HTT)	6.38E-25
N-myc proto-oncogene protein (MYCN)	2.95E-20
CD 437 (apoptosis inducer)	2.98E-20
Histone deacetylase 4 (HDAC4)	6.11E-20
5-fluorouracil (antitumor agent)	4.57E-17
sirolimus (Rapamycin; antitumor agent)	3.99E-16
Fragile X mental retardation 1 (FMR1)	9.41E-16

Supplementary Table 3. Top canonical pathways (IPA) coordinately deregulated in mouse *Sst*-expressing neurons treated with chronic corticosterone relative to non-stressed neurons.

Ingenuity Canonical Pathways	P-Value	Ratio	De-regulated Molecules [a]	
			Up	Down
Eukaryotic translation initiation factor 2	1.74E-04	11.9%		NRAS,RPL36A/RPL36A-HNRNPH2,RPL27,RPL17,PDPK1, EIF4G3,RPL23A,RPL9,RPL35A,RPLP0,RPS4X,UBA52, EIF4A3,RPS15,RPL19,Rn18s,EIF3A,RPL38,MAP2K1,RPL18, RPL31,RPL29,RPL13,EIF3K
tRNA Charging	1.30E-03	9.9%	MARS2	LARS,CARS2,GARS,HARS,AARS,MARS,FARSB
Hypoxia Signaling	1.38E-03	16.2%		UBE2L3,UBE2J1,CREB1,UBE2V1,CSNK1D,UBE2V2,CDC34, UBE2S,NFKBIB,VHL,UBE2I
Cholecystokinin/Gastrin- mediated Signaling	2.09E-03	13.2%	IL1F10, IL36G	MAP2K4,NRAS,SRF,MEF2A,GNAQ,CCK,PRKCI,MEF2D, PLCB1,MAP2K1,MAP2K5,CCKBR
Salvage Pathways of Pyrimidine Ribonucleotides	3.33E-03	11.5%		BRAF,MAP2K4,NME3,CDK18,NME1,SGK1,PRKAA1, CSNK1D,AK4,UCK2,HIPK1,MAP2K1,DYRK1A
Relaxin Signaling	6.02E-03	9.8%		PDE2A,GUCY1A3,PDE10A,GNAQ,PDE4A,GNAZ,PDE4D, RAP1A,BRAF,CREB1,GNAO1,GUCY1A2,NFKBIB,NPR2, MAP2K1,GNG12
Glycoaminoglycan-protein Linkage Region Biosynthesis	8.80E-03	18.8%		XYLT1,B3GAT1,B3GAT3
UVC-Induced MAPK	1.08E-02	8.7%		MAP2K4,BRAF,PRKCI,NRAS,SMPD4,MAP2K1,MAPK11
Huntington's Disease Signaling	1.13E-02	13.2%		MAP2K4,CAPN5,MAP2K7,SGK1,IFT57,GNAQ,NAPG, PDPK1,UBE2S,STX1A,VTI1B,RPH3A,PRKCI,DNAJC5,CREB1, HTT,IGF1R,PLCB1,STX16,NCOR2,RASA1,GNG12

Genes were tested for differential expression between corticosterone-treated and control groups. Statistical significance for differential expression was reached at fold-change > 20% and *p*<0.05. The resulting signature was submitted to IPA to test for over-representation of canonical pathways. The p-value was calculated by right-tailed Fisher's exact tests (Fisher 1922). The ratio was calculated by the number of differentially expressed genes, divided by total number of genes that make up in a given pathway.

References

1.   Zeyda T, Diehl N, Paylor R, Brennan MB, Hochgeschwender U. Impairment in motor learning of somatostatin null mutant mice. *Brain Res* 2001; **906**(1-2)**:** 107-114.

2.   Taniguchi H, He M, Wu P, Kim S, Paik R, Sugino K *et al.* A resource of Cre driver lines for genetic targeting of GABAergic neurons in cerebral cortex. *Neuron* 2011; **71**(6)**:** 995-1013.

3.   Surget A, Wang Y, Leman S, Ibarguen-Vargas Y, Edgar N, Griebel G *et al.* Corticolimbic transcriptome changes are state-dependent and region-specific in a rodent model of depression and of antidepressant reversal. *Neuropsychopharmacology* 2009; **34**(6)**:** 1363-1380.

4.   Sibille E, Pavlides C, Benke D, Toth M. Genetic inactivation of the Serotonin(1A) receptor in mice results in downregulation of major GABA(A) receptor alpha subunits, reduction of GABA(A) receptor binding, and benzodiazepine-resistant anxiety. *J Neurosci* 2000; **20**(8)**:** 2758-2765.

5.   Guilloux JP, Seney M, Edgar N, Sibille E. Integrated behavioral z-scoring increases the sensitivity and reliability of behavioral phenotyping in mice: relevance to emotionality and sex. *J Neurosci Methods* 2011; **197**(1)**:** 21-31.

6.   Weissman MM, Bland R, Joyce PR, Newman S, Wells JE, Wittchen HU. Sex differences in rates of depression: cross-national perspectives. *J Affect Disord* 1993; **29**(2-3)**:** 77-84.

7.   Lin LC, Lewis DA, Sibille E. A human-mouse conserved sex bias in amygdala gene expression related to circadian clock and energy metabolism. *Mol Brain* 2011; **4:** 18.

8.   Moreno JA, Radford H, Peretti D, Steinert JR, Verity N, Martin MG *et al.* Sustained translational repression by eIF2alpha-P mediates prion neurodegeneration. *Nature* 2012; **485**(7399)**:** 507-511.

9.   Ma T, Trinh MA, Wexler AJ, Bourbon C, Gatti E, Pierre P *et al.* Suppression of eIF2alpha kinases alleviates Alzheimer's disease-related plasticity and memory deficits. *Nat Neurosci* 2013; **16**(9)**:** 1299-1305.

10.   Moreno JA, Halliday M, Molloy C, Radford H, Verity N, Axten JM *et al.* Oral treatment targeting the unfolded protein response prevents neurodegeneration and clinical disease in prion-infected mice. *Sci Transl Med* 2013; **5**(206)**:** 206ra138.

11.   Kim HJ, Raphael AR, Ladow ES, McGurk L, Weber RA, Trojanowski JQ *et al.* Therapeutic modulation of eIF2alpha phosphorylation rescues TDP-43 toxicity in amyotrophic lateral sclerosis disease models. *Nat Genet* 2014; **46**(2)**:** 152-160.